

## 3-D and 3-C seismic data analysis at Cold Lake, Alberta

J. Helen Isaac and Don C. Lawton

### ABSTRACT

3-D and 3-C seismic data have been acquired at Cold Lake, Alberta, where Imperial Oil Resources Ltd. is producing bitumen from the Clearwater Formation by means of cyclical steam stimulation of the reservoir. The data are intended for use in monitoring those changes in reservoir characteristics that can be detected seismically. The two time-lapse 3-D surveys were reprocessed in 1993 to minimise the differences between them above the reservoir. Analysis of these differences show that they are very small so that differences now observed within the reservoir section on the two surveys may be attributed to changes in reservoir conditions at the times of acquisition. 3-D inversion of the data using an extracted wavelet shows zones of low velocity at about the level of the perforations in the 1992 data, which were acquired during the steam cycle. The 1990 data, acquired during the production cycle, have low velocity zones, interpreted to be gas saturated zones.

A multicomponent survey acquired in 1993 with a *P*-wave source is being processed. The vertical channel data have been processed as regular *P-P* data through a processing stream that includes post-stack deconvolution and post-stack time migration. Shot gathers of the radial channel data show a great deal of incoherent noise but receiver gathers reveal coherent energy trains, including some *P*-wave energy. Preliminary processing indicates that there are very large receiver statics to be applied to the radial channel and that *P-SV* stacking velocities are low. Velocity data obtained from a well dipole survey indicate a  $V_p/V_s$  ratio of 2.4 above the reservoir and about 2.04 within the reservoir. It is anticipated that the introduction of steam into the reservoir will affect the  $V_p/V_s$  ratio. If the converted wave energy on the radial channel can be identified and processed to stack, this stacked section and the vertical channel stacked section may be used to determine changes in  $V_p/V_s$  along the line.

### INTRODUCTION

Two 3-D and two 3-C seismic surveys have been acquired by Imperial Oil Resources Ltd. as part of a reservoir monitoring program at Cold Lake, Alberta. The Upper Mannville Clearwater sandstones are saturated with highly viscous bitumen, which is being produced by an enhanced oil recovery (EOR) process. The Clearwater sands at Cold Lake have a gross thickness of 55 m within the depth interval 420-475 m. They have an average porosity of 32% and permeability of 1 darcy. At the D3 and AABBW pads (Figure 1), the reservoir is undergoing cyclical steam stimulation (CSS). Steam is injected into the reservoir through directionally drilled injection/production wells for 30-50 days and the oil is produced through the same wells for up to one year. In order to produce the reservoir efficiently, it is necessary to maximise the volume of sand swept by the steam. This entails knowing the volumetric distribution of the steam in the reservoir and of the bitumen production. One method of investigating the distribution of steam in the reservoir is from the interpretation and analysis of reflection seismic data. Laboratory measurements have shown that raised reservoir temperatures

associated with certain EOR processes can cause a significant reduction in the compressional wave velocity of the reservoir (Nur et al., 1984; Nur, 1987). The application of seismic methods in EOR projects has been discussed by several authors (e.g., Macrides and Kanasewich, 1987; Laine, 1987; Paulsson et al., 1992) and the use of seismic methods in this particular project has been demonstrated (Eastwood et al., 1994).

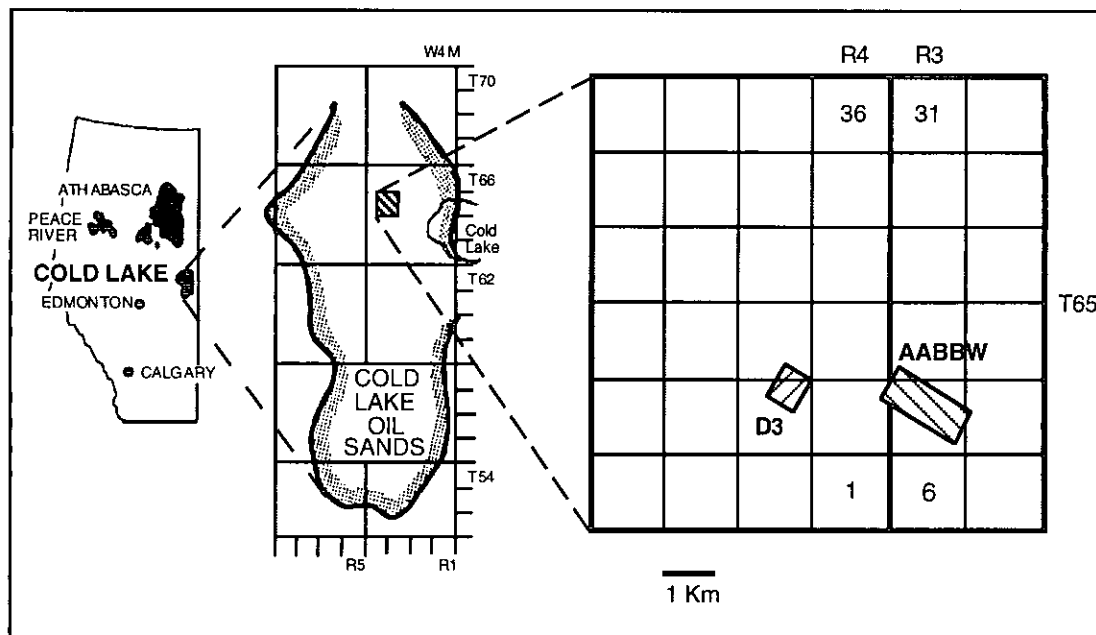


FIG.1. The study area at Cold Lake. 3-D data over the D3 pad and 3-C data at the AABBW pads are being analysed. (after Harrison et al., 1981)

Two 3-D seismic surveys were acquired over the D3 pad in January 1990 and April 1992. It was anticipated that, by conducting two such time-lapse seismic surveys, the change in reservoir conditions caused by the injection of steam may be observed. The lower interval velocities resulting from the presence of steam or of gas brought out of solution by the steam should be detectable using seismic imaging techniques. Observed differences in seismic data between the two surveys in the reservoir zone may be attributed to differences in reservoir conditions at the times of acquisition of the surveys. These differences may be mapped to give a volumetric picture of the parts of the reservoir affected by steam injection. The data were reprocessed (Isaac and Lawton, 1993) to minimise the differences between them above the reservoir zone. Analysis of the two data sets and of the differences between them has been undertaken and is discussed in this paper.

An extracted wavelet was obtained and used in the 3-D inversion of the two data volumes. The inversion results show zones of low velocity within the reservoir in 1990 and 1992 and lower interval velocities throughout the reservoir in 1992. The low velocity zones are thought to represent gas saturated zones in the 1990 data and steamed zones in the 1992 data. Also apparent are the presence of high velocity zones, interpreted to represent tight streaks.

Two multicomponent (3-C) surveys were acquired over the AABBW pads in November 1993 and May 1994. Preliminary processing results from the first survey indicate that there are extremely large receiver statics to be applied to the radial component.

### 3-D SEISMIC DATA AT D3 PAD

#### Seismic data - well-log correlation

In order to identify reflectors on the seismic data, a suite of synthetic seismograms was made. Figure 2 shows the identification of seismic reflectors based on the correlation at the location of OB5. It is seen that some degree of stretch is necessary to tie the Clearwater and McMurray reflectors to the sonic log. Tests were undertaken to tie the synthetic to a series of phase-rotated panels of seismic data but there was no improvement over the zero-phase data. The logs were acquired prior to the commencement of CSS so may not now be an accurate measure of the rock properties. Although the response to tight streaks would not have been altered, the presence of gas brought out of solution by the CSS process may affect the composite seismic response.

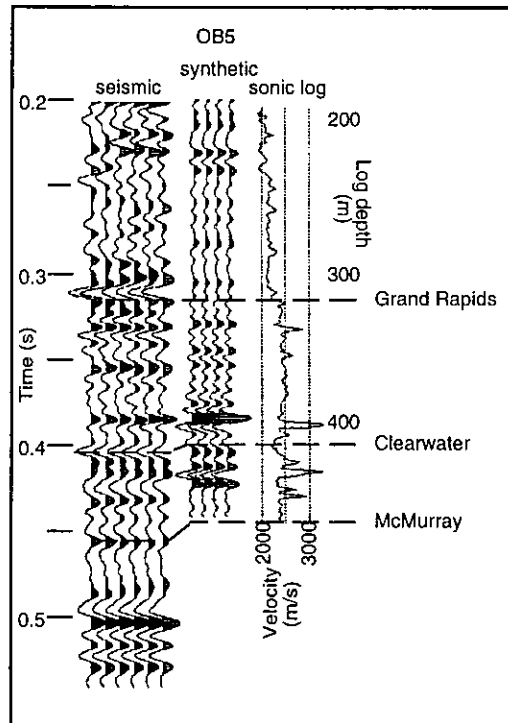


FIG. 2. Correlation of seismic reflectors based on the OB5 synthetic seismogram.

To identify better the reflections within the reservoir zone and for use in 3-D inversion, a wavelet extraction from the seismic data was done. It was hoped that synthetic seismograms created using a wavelet extracted from the data would correlate better with the data than those created using a standard Ormsby wavelet, as used in Figure 2. Several extractions were done using the sonic log from well OB5 and nine traces of seismic data from near that well's location.

The wavelet extraction program used was WAVX, which utilises the Wiener-Levinson method of wavelet estimation. A wavelet was extracted for each of the nine traces and the wavelets summed after tapering to shorten and smooth them. The ideal window to use for the sonic log-seismic correlation should be one in which the reflectivity series is generally of low amplitude but with sparse, high amplitude events

(Brown et al., 1988) at a spacing comparable to the length of the wavelet (Lazear, 1984). The window should also cover data with high signal/noise ratio. In the study area the portion of log available is limited because of the shallow depth of the reservoir zone (420-475 m). The window was selected to exclude the high amplitude events above the Colorado Formation and to avoid the noisy, shallower seismic events. The final window used was one from about 130 m to 475 m on the OB5 sonic log. Too short a window gave poor results, probably because the wavelet and window were of comparable length.

Parameters such as wavelet length and window length were varied, as was the amount of editing done to the wavelet. Synthetic seismograms for the wells OB1, OB2, OB5 and D3-8 were created with several extracted wavelets and the final wavelet selected was that which gave the best synthetic/seismic tie for all these wells (Figure 3). Wells OB5, OB2 and OB1 are vertical observation wells and D3-8 is a deviated well. The log shown for D3-8 is a TVD log. The wavelet, displayed in Figure 3, is 100 ms long and is composed of a primary event followed by a secondary one 25 ms later. This second event could be the result of a reflection at the ground surface, 10 m above the geophone level, in the low velocity layer. The well-seismic correlation is based on a tight streak in the Grand Rapids formation at about 400 m. This tight streak is observed to be present on the logs from OB5 and D3-8 but not from OB2 or OB1. The tight streak correlates well to a peak observed on the seismic data at about 0.38 s, which is present at the location of OB5 and D3-8 but not at OB2 or OB1. The location on the seismic data of the projection of the deviated D3-8 wellbore was calculated using the known BHL location, angle of deviation and depths of the BHL and tight streak. The well log/seismic correlation shows that it is not easy to relate seismic peaks directly to tight streaks because of the composite wavelet and response.

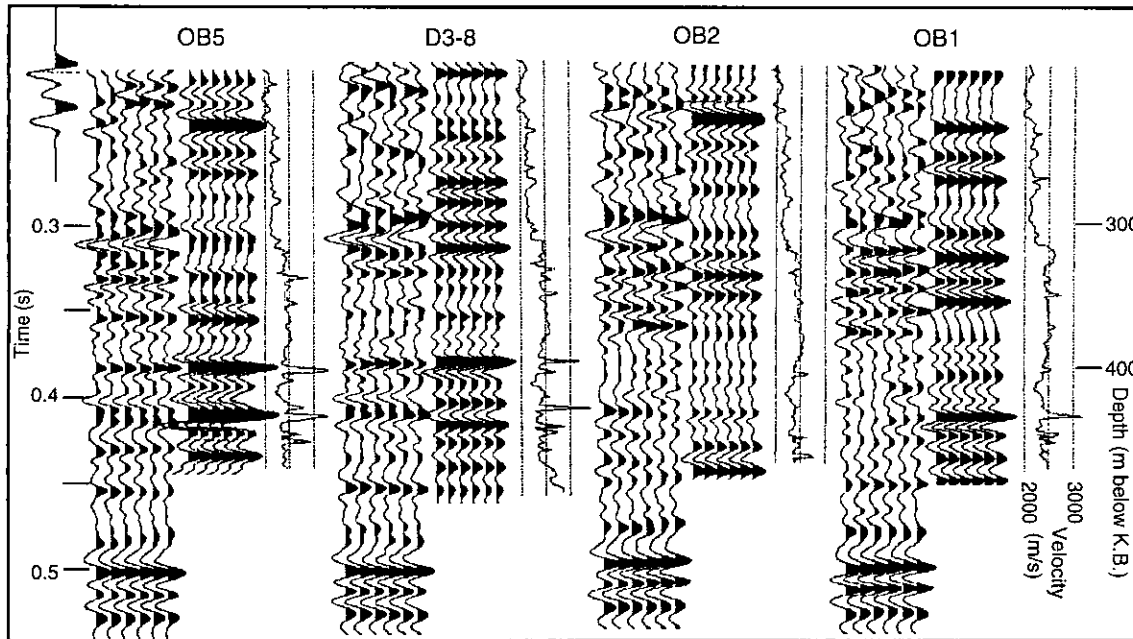


FIG. 3. Correlation of seismic data using the extracted wavelet and four wells.

### 3-D Seismic data analysis

The time-lapse 3-D seismic surveys were acquired in 1990 and 1992 and it was anticipated that temporal changes in reservoir conditions could be inferred from the seismic character and attribute differences observed between the two processed surveys. If any observed differences within the reservoir zone between the two processed data volumes are to be ascribed to temporal changes in the reservoir and not to data processing artifacts, then it is necessary to ensure that the differences between the two volumes are kept to a minimum above the reservoir zone, where conditions have not been affected by the introduction of steam into the reservoir. The two surveys were reprocessed together, using identical processing parameters, with the objective of keeping the differences between them above the reservoir zone to a minimum. The reprocessing procedure was discussed by Isaac and Lawton (1993).

Figure 4 shows examples of a line from the migrated reprocessed data, selected from the central part of the 1990 and 1992 surveys, respectively.

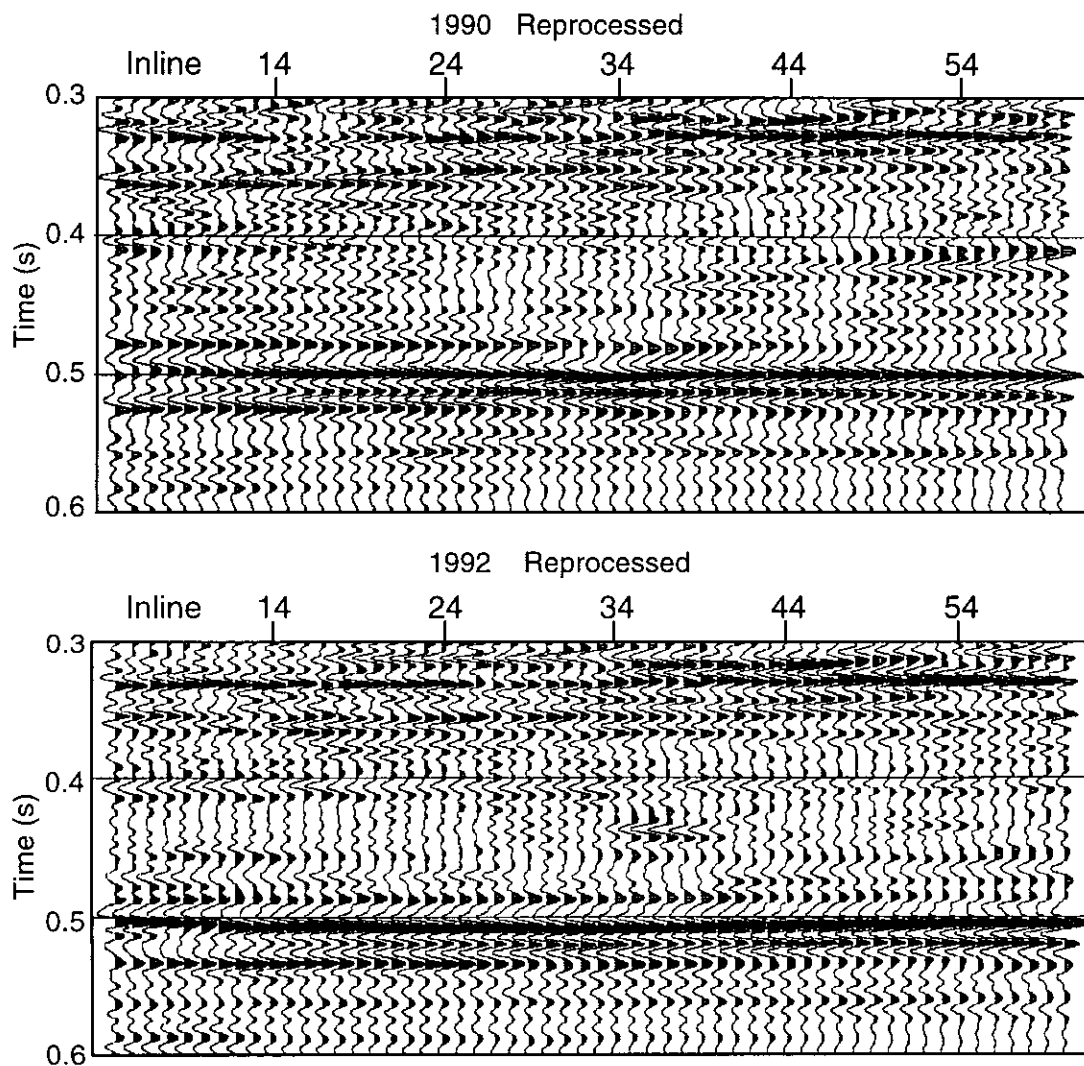


FIG. 4. Reprocessed, migrated crossline 50 from the centre of the 1990 and 1992 data volumes.

The displayed line is a southwest-northeast crossline, the location of which is shown in Figure 6. The end portions of the lines, where data quality is poor because of low fold, are not displayed and the data have been bandpass filtered between frequencies of 25/30-100/120 Hz. The top of the Clearwater Formation is identified by the trough which occurs just after 0.4 s and the top of the Devonian is the peak at about 0.5 s.

Comparison of the 1990 and 1992 lines in Figure 4 reveals examples of seismic character differences within the reservoir zone, which extends from 0.405 s to 0.450 s. Two major differences can be observed in this interval. A high amplitude event can be seen on inline traces 34 to 40 on the 1992 line, at a time of 0.435 s. This event, not seen on the 1990 line, is interpreted to be due to the presence of steam in the reservoir during the acquisition of the 1992 survey. The presence on the 1990 line of a high amplitude event at 0.415 s over traces 40 to 60, which is absent on the 1992 line, also indicates a change in reservoir conditions. It is possible that it is due to the localised presence of a gas saturated zone. These zones were present in 1990 but in 1992 the presence of steam precluded the existence of gas, except in very thin zones (Eastwood, 1994). The traveltimes for the Clearwater-Devonian interval are almost the same for the 1990 and 1992 data. It is thought that the low interval velocity of the gas saturated zones in 1990 has the same effect on interval transit times as the lower overall interval velocity seen in the 1992 data. Observation of the Clearwater-Devonian interval in Figure 4 reveals an increased interval transit time for the 1992 line. This increase is attributed to the reduction in interval velocities in the steamed zone in 1992. A comprehensive analysis of these observed traveltime anomalies is discussed by Eastwood et al. (1994).

The differences between the 1990 and 1992 migrated data volumes are shown in Figure 5 for the same crossline as in Figure 4. From a time of 0.300 s to the top of the reservoir zone at 0.405 s, the residual amplitudes are minimal but increase considerably once the reservoir is entered. The high amplitude residual observed at the Devonian level in Figure 5 is due to differences in reflection traveltimes between the 1990 and 1992 surveys rather than the differences in the amplitude of the Devonian event. The Devonian arrival times are different across all the displayed line but this effect is seen to be localised on other lines in the survey. This indicates that the Devonian arrival times have not been delayed consistently over the survey area. A high amplitude residual event is present on the right end of the line at a time of 0.415 ms. This event corresponds to the high amplitude event observed at the right end of the 1990 line and which is absent on the 1992 line in Figure 4. The fairly high amplitude trough observed at 0.435 ms over inlines 34-40 in Figure 5 is the residual of the event seen on the 1992 line and absent on the 1990 line in Figure 4. Seismic amplitude differences are clearly evident in and below the reservoir zone and, since the residuals above this zone have been minimised, we may with confidence state that these differences are due to temporal changes in reservoir conditions and analysis of them can be initiated with validity.

Although the amplitude differences in the reservoir zone in Figure 5 are of limited extent, the traveltime delay in the Devonian exists across almost the entire line. The delay is only very small underneath the interpreted 1990 gas zone. We interpret that we are observing two effects on seismic data of changes in reservoir conditions. The first effect is a decrease in interval velocity in the reservoir zone caused by the presence of steam and the second is a change in seismic amplitude caused by a localised change in reflectivity. These localised changes are interpreted to be due to the presence of gas in 1990, absent in 1992, and the presence of steam in 1992, absent in 1990.

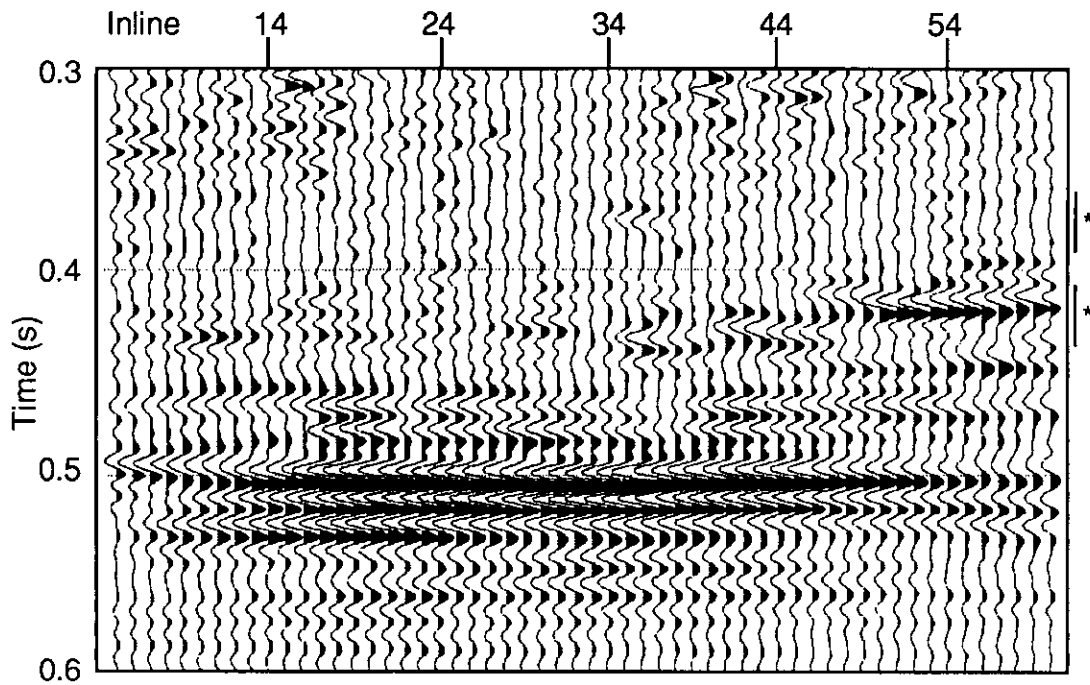


FIG. 5. The differences between the 1992 and 1990 line displayed in Figure 4. The asterisks denote the time zones used in the rms amplitude analysis discussed in the text.

Statistical analysis of the residual and original data amplitudes was also undertaken. The mean absolute amplitude and standard deviation were calculated over selected time intervals from the residual 3-D data volume and the mean absolute amplitude from the reprocessed 1990 data volume. Some of the results are presented in Table 1 and the values show statistically that the residual amplitudes above the reservoir zone are much lower than those within the reservoir interval.

Data set	Time window (ms)	Mean Amplitude	Standard Deviation
1992-1990 residual	350-400 (above reservoir)	3550	285
1992 -1990 residual	420-520 (within and below reservoir)	12251	983
1990 reprocessed	350-400 (above reservoir)	11642	
1990 reprocessed	420-520 (within and below reservoir)	11770	

TABLE 1. Statistical analysis of the amplitudes.

The residual data volume was loaded onto a workstation and preliminary analysis done using Landmark® software. RMS amplitudes for 30 ms zones above and within the reservoir were calculated. Time zones selected were 0.360-0.390 s for the zone above the reservoir and 0.005-0.035 s below the Top Clearwater event for the zone within the reservoir (Figure 5). Figure 6 displays the spatial variation in map view of the rms amplitudes.

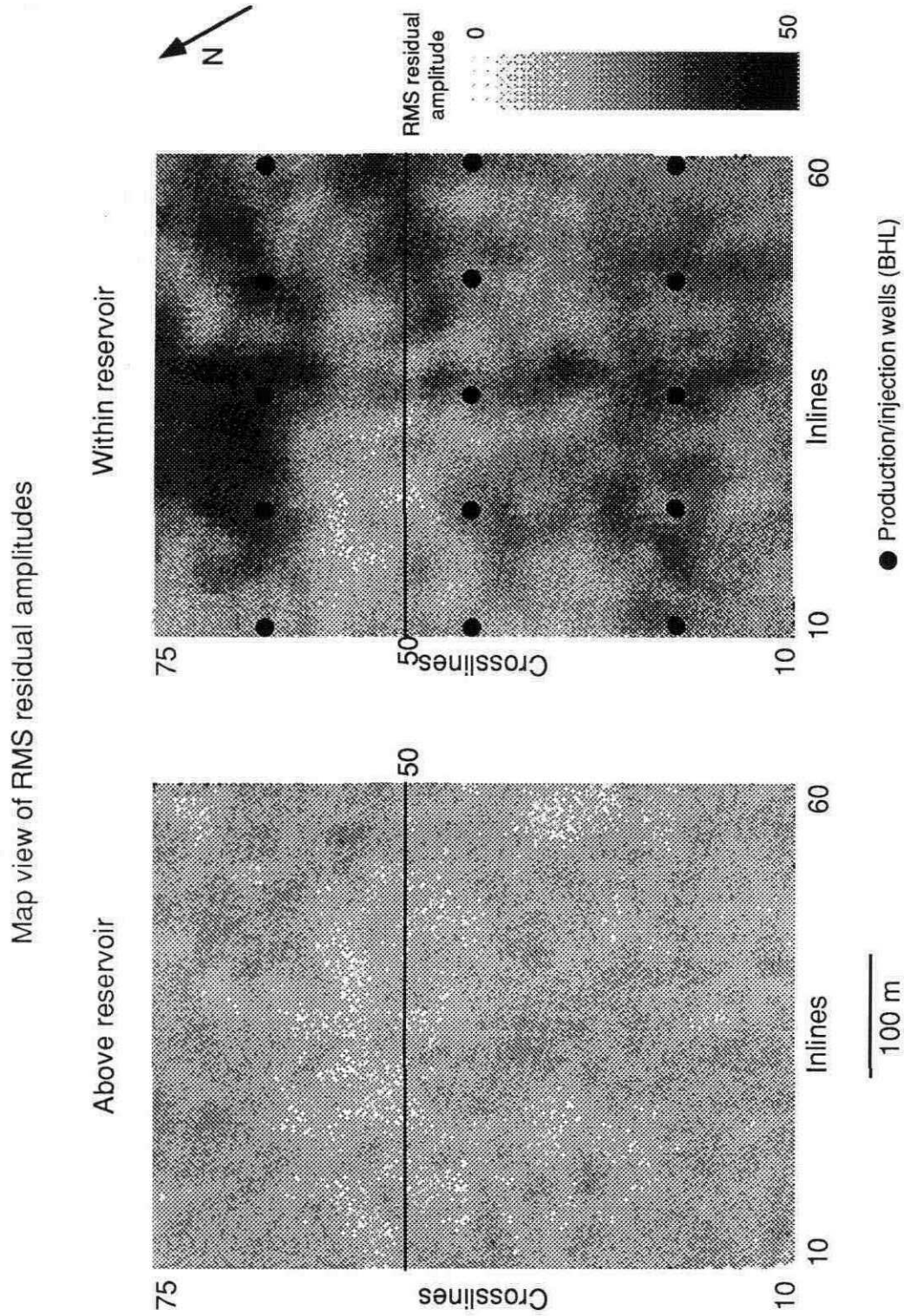


FIG. 6. Map view of the rms amplitudes above and within the reservoir.

The data were scaled from 0 to 50, where white represents 0 (low residual amplitudes) and black 50 (high residual amplitudes). The map view shows clearly lower residual rms amplitudes from the data above the reservoir compared with those from the data within the reservoir. On the map representing the reservoir zone, the darker greys indicate areas of greatest residual differences, where it is interpreted that reservoir conditions have changed due to the presence of steam. The dark patch at the right of the map shows the areal extent of the high amplitude anomaly seen at 0.415 s on the right end of crossline 50 in Figures 4 and 5 (discussed earlier). Another anomaly observed in Figure 5, at 0.435 s, maps as a dark grey linear trend across the middle of the map, running in a southwest to northeast direction. It is a possible indication of communication between the wells in this direction. Some of the changes in reflectivity are thought to be due to gas saturated zones in 1990 and others due to steamed zones in 1992. Overlying tight zones inhibit the vertical migration of the steam. Future work includes trying to separate the two reflectivity effects.

### **3-D Inversion**

The 1990 and 1992 data were 3-D inverted using Strata3d. Sonic and density logs from OB1, OB2 and OB5 and the extracted wavelet were imported into the program to provide control points. The Clearwater, McMurray and Devonian time picks were exported from Landmark into an ASCII file and imported into Strata3d. A blocky inversion was done over the time interval 350-500 ms using an interval time of 6 ms. Figure 7 shows the results of the inversion at the location of the OB5 observation well (which gave the best well-seismic tie). Displayed are the synthetic seismogram created using the extracted wavelet with its tie to the seismic data, the 1990 inversion and the 1992 inversion for inline 38. The velocity scale is from 2000 m/s to 2700 ms/ with light shades representing low velocities and dark shades representing high velocities.

Both inversions show the same high velocity, strong tight zone in the Grand Rapids Formation at about 380 ms and in the Clearwater Formation at about 412 ms but cannot resolve the minor tight streaks at 424ms and 430 ms on the sonic log. The Grand Rapids tight streak is about 4 m thick while the others are only about 1 m thick. The two tight streaks at 410 ms and 414 ms on the sonic log are only 3 m apart and generate a composite response on the seismic data and the inversion.

The depths of the perforations in the injection wells varies slightly from well to well but are at an average of 38-54 m below the top of the Clearwater Formation. This translates to a two-way traveltime of 36-40 ms. This time corresponds exactly to the very low velocity zone (white) seen to the left of OB5 on the 1992 inversion. It is interpreted that the extent of the low velocity zone on the inversion denotes the extent of the steamed zone that is inhibited from permeating up through the reservoir by the overlying tight streaks. Overall, velocities calculated from the 1992 data are lower than those from the 1990 data.

In Figure 8 are displayed the seismic data and inversions for line 35. On traces 59-66 on the 1990 inversion is a low velocity zone at about 415-420 ms. This is believed to be a localised gas zone, as referred to earlier in the text. The interval transit times between the Clearwater and McMurray events do not change here. Lower interval velocities in the 1992 data cancel the velocity effect of the 1990 gas zone. From traces 47 to 58 on the 1992 line we see a low velocity zone at about 428-432 ms. This is interpreted to be a steamed zone, underlying a tight zone (compare with Figure 7). Note the delayed arrival time of the McMurray event, especially over traces 52-57.

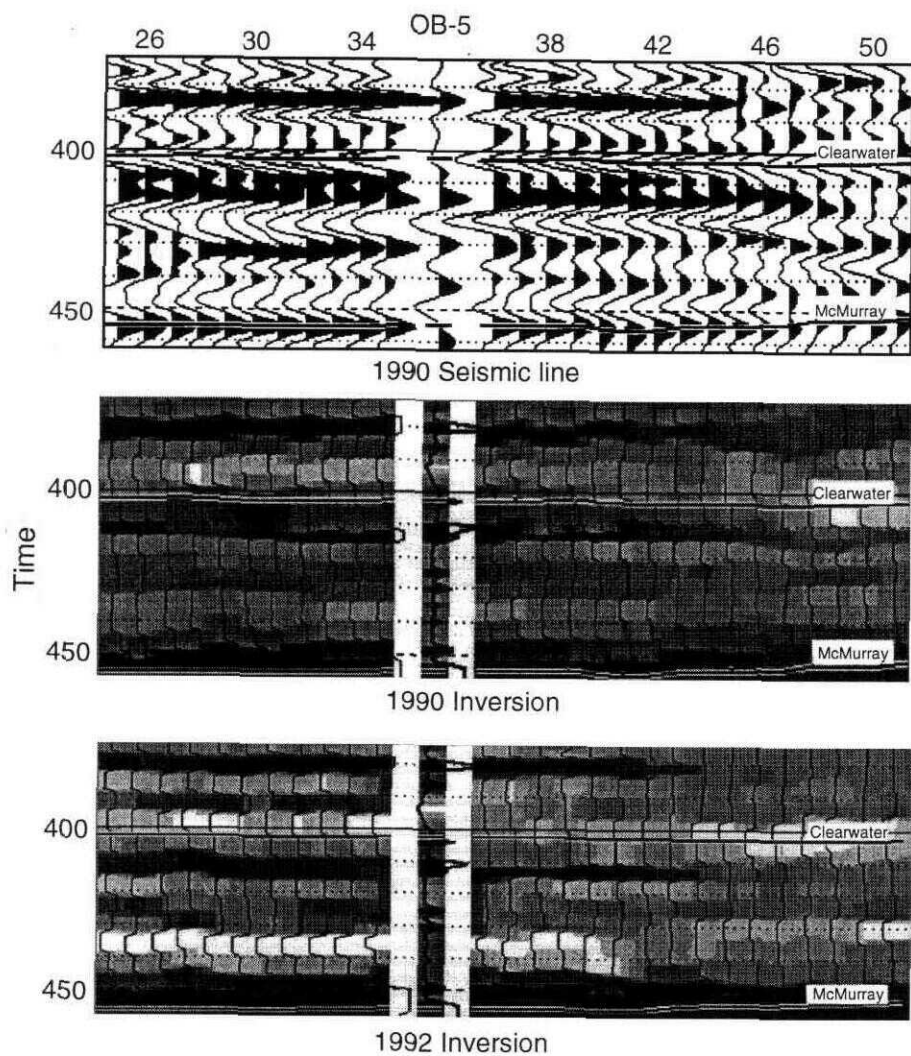
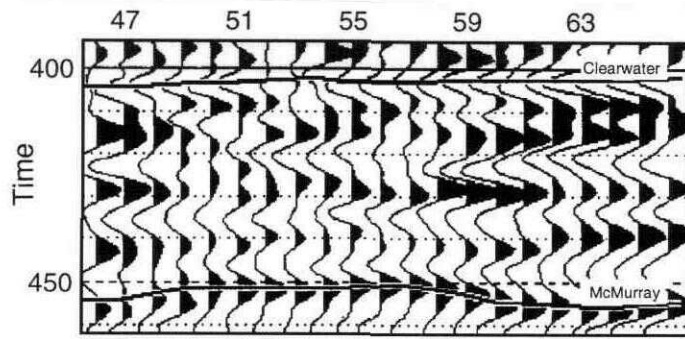
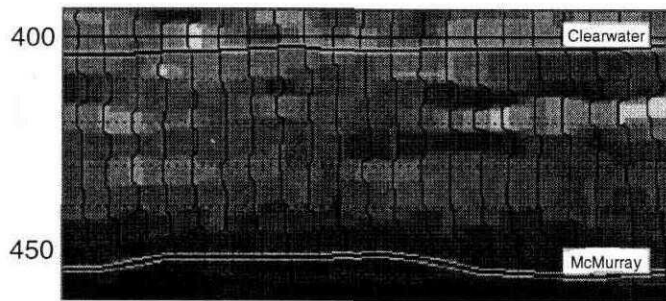


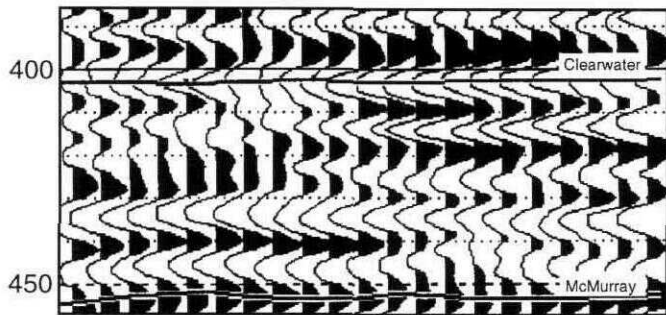
FIG. 7. Seismic line 38 with the synthetic seismogram tie to well OB5 and the results of the 3-D inversion for the 1990 and 1992 data.



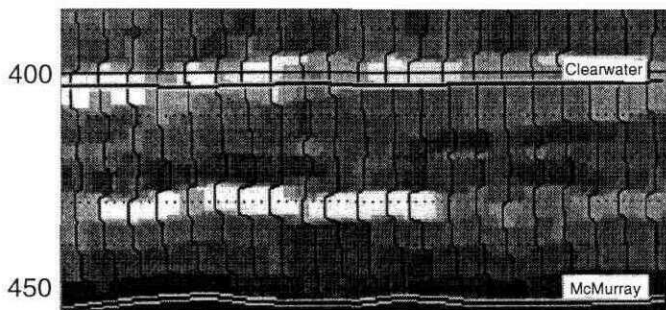
1990 Seismic line 35



1990 Inversion



1992 Seismic line 35



1992 Inversion

FIG. 8. The inversion for line 35.

### 3-C SEISMIC DATA

The use of multicomponent seismic data analysis in petroleum exploration has started to become of more interest to explorationists. Analysis of *P*- and *S*-wave data can be applied to the estimation of rock properties such as lithology, porosity and fluid content (Domenico, 1984; Winterstein, 1986). Analysis of *S*-wave splitting may be used to determine fracture orientation (Crampin, 1985; Martin and Davis, 1987). The application of multicomponent seismic methods in exploration is well documented in, e.g., Dohr (1985) and Tatham and McCormack (1991).

Converted wave seismic data analysis has been used to determine stratigraphic variations within sand/shale sequences (Baltenspergen and Bay, 1990) but has not yet, to our knowledge, been applied to heavy oil reservoir characterisation problems. The potential for using multicomponent methods at Cold Lake has been investigated. Macrides and Kanasewich (1987) measured a Poisson's ratio as high as 0.4 in the steam-invaded zones of Cold Lake oil sands compared with a value of 0.3 in uninvaded zones. They suggested that high Poisson's ratio indicates a zone dominated by steam condensate.

Eastwood (1993) compared theoretical model predictions of seismic wave propagation with results obtained from experiments on ultrasonic velocities in sands from the D3 area. His theoretical models predicted a 15% decrease in the *P*-wave velocity and less than 1% increase in the *S*-wave velocity of the sands for a temperature rise from 22°C to 125°C. The theoretical and experimental results for *P*-wave velocities agreed to within 5% for this temperature range; experimental results for *S*-wave velocities were not obtained. For a temperature increase of 22°C to 200°C, the theoretical modelling predicted a major fall in *P*-wave velocity from 2130 m/s to 1660 m/s and a minor rise in *S*-wave velocity from 1180 m/s to 1190 m/s. The results of experimental studies by some authors (Tosaya, 1987; Wang and Nur, 1988) show, however, that the *S*-wave velocities also decrease with increasing temperature. The results of Eastwood's work imply that  $V_p/V_s$  or Poisson's ratios determined at the AABBW pads may be used to determine temperature variations in the reservoir. Other factors that affect the  $V_p/V_s$  ratio, such as porosity and lithology, change much less significantly than the temperature.

#### 3.2 Field Acquisition

Two surveys of multi-component (3-C) seismic data were acquired over the AABBW pads at Cold Lake (Figure 1) during the acquisition of 3-D seismic surveys. The first survey was in November 1993, at the peak of the injection cycle, and the follow-up survey in May 1994, during the production cycle.

One surface receiver line of 3-C geophones was laid out to coincide with a source line (line 470) and these geophones recorded data from the shots along seven source lines in the 3-D survey. Figure 9 shows the layout of the survey. The source and receiver station interval was 16 m and the source lines spaced 125 m apart. The receiver line and source lines 468 to 473 were 1800 m long, (114 stations each) and line 474 was 750 m (48 stations). The source was 0.125 kg of dynamite buried 12 m deep and a total of 732 live shots was recorded.

Each record of 342 traces was separated into three shot gathers representing the three components: vertical, orthogonal to the direction of line 470 and along the direction of line 470.

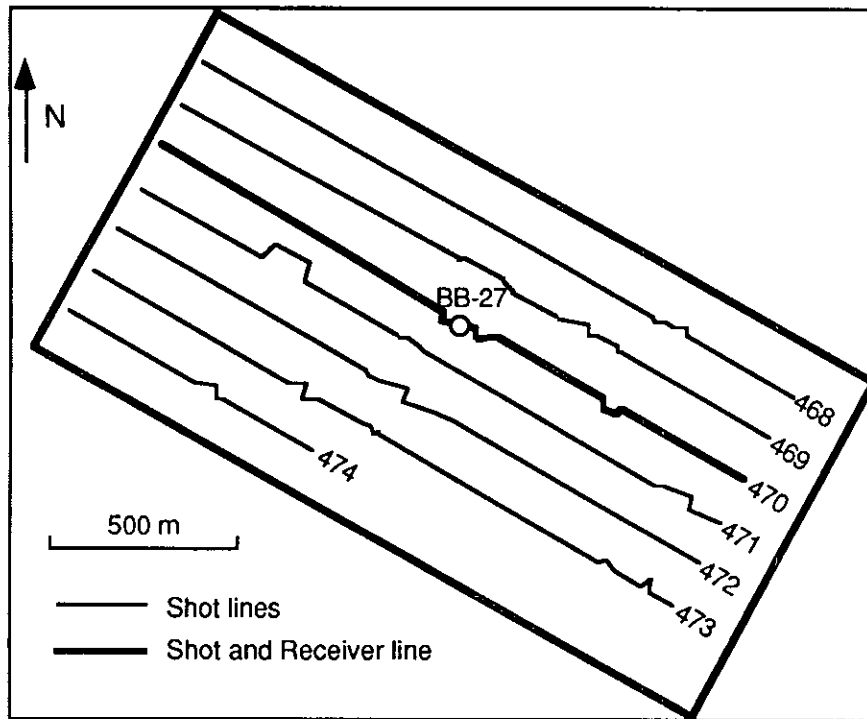


FIG. 9. layout of the 3-C survey

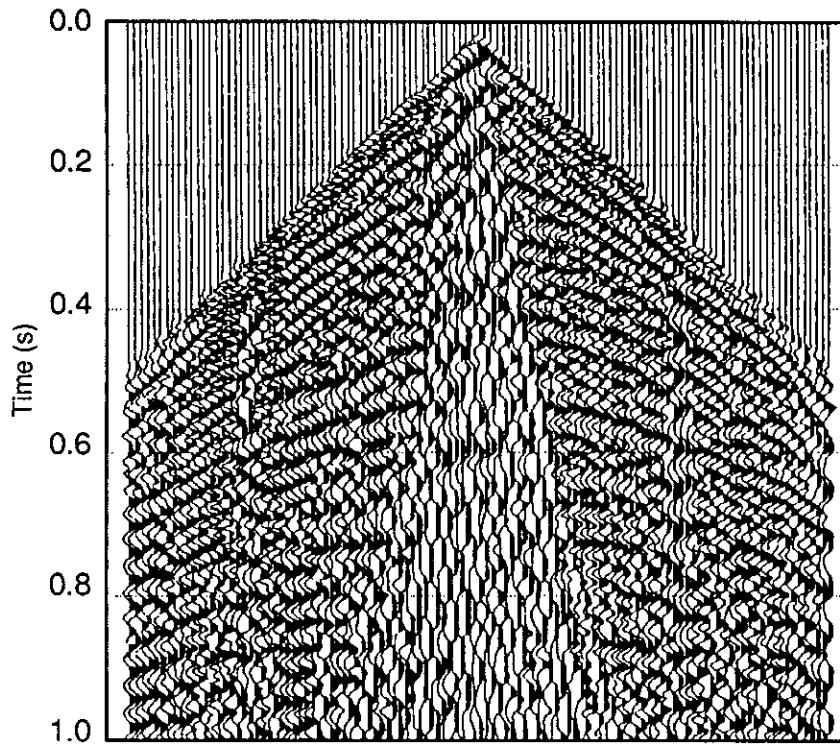
### 3-C Data Processing

#### Vertical channel

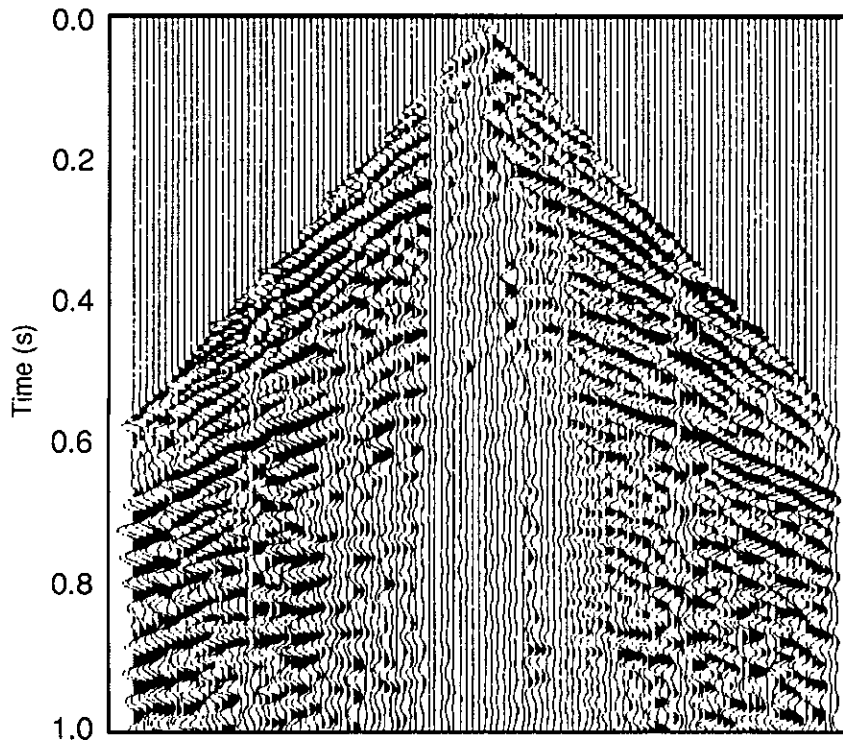
The vertical channel data were processed using ITA "Insight" software with a 3-D geometry, since the source and receiver lines were not coincident, apart from line 470. Each line was processed using the same processing scheme with the same parameters where appropriate.

After first breaks had been picked, refraction statics were calculated using GLI3D. The statics were calculated independently for each line to investigate the robustness of the program, as the receiver statics should be common for each line. The calculated receiver statics were found to vary only very slightly from line to line; by at most 5 ms and usually only one or two ms, giving confidence in the validity of the calculated values. Refraction statics calculated using ITA's Ref3d were very similar to those calculated by GLI3D.

Many of the shot records were contaminated with low-frequency, high amplitude noise, some of which was shot-generated and some caused by external sources. To remove this noise it was decided to  $f-k$  filter the NMO-corrected shot gathers, discriminating against dipping events. Figure 10 shows a raw shot gather from line 470 and the same record after geometric spreading compensation, refraction and residual statics corrections and  $f-k$  filtering. Partial processing of the unfiltered data was necessary to determine the residual statics and stacking velocity functions.



a. Raw vertical channel shot gather from line 470



b. Filtered vertical channel shot gather

FIG. 10. a. A shot gather of the vertical channel from line 470. b. The same gather after refraction statics and  $f-k$  filtering.

Refraction and residual statics were applied to the raw shot records to correctly position events along their moveout hyperbolae then the records were NMO-corrected.  $F-k$  filtering was done on these NMO-corrected records to discriminate against high wavenumber and dipping events then the NMO correction was removed. The shot gathers were then processed through a standard processing sequence which included post-stack deconvolution and post-stack time migration.

### Radial channel

The presence of anisotropy in the subsurface can cause an upcoming shear-wave to split into fast and slow components and this effect has been observed on reflection seismic data (Lynn and Thomsen, 1986). For converted wave data, energy may then be recorded on both horizontal channels and each channel may contain both fast and slow components. If the natural coordinate system can be determined then the recorded components can be rotated into this system.

An attempt was made to calculate the directions of these components by cross-correlation of two corresponding records of horizontal components (Harrison, 1992) from line 470. Shot - receiver azimuths along this line did not vary except near the two or three out-of-position shots. These traces with azimuths much different from the orientation of the line were, however, unusable anyway because of the great amount of shot noise present. Several records along the line were selected for the rotation analysis but no consistent value could be calculated. It is surmised that either there is no shear-wave splitting in this area or the receiver line lies along a natural coordinate axis or that the level of noise in the data is too high to permit cross-correlation of shear events. The direction of maximum horizontal stress (a natural coordinate axis) is  $30^\circ$  to  $45^\circ$  from North in the Cold Lake area (Bell et al., 1994). The seismic lines are oriented at an angle of  $120^\circ$  so it is feasible that they are coincident with a natural coordinate axis.

Because mode-converted  $P$ - $SV$  data are polarised in the same vertical plane as the incident  $P$ -wave, each corresponding pair of traces from the orthogonal and inline shot gathers had to be rotated into components oriented in the source-receiver plane (radial) and orthogonal to that plane (transverse). This angle of rotation was unique for each source-receiver azimuth.

The polarity of the trailing spread was reversed so that all the traces in a gather would have the same polarity. Geometric spreading compensation was applied using estimated  $P$ - $SV$  stacking velocities, total two-way travel time and the near-surface  $P$ -wave velocity (Harrison, 1992). The  $P$ - $P$  stacking velocities for each line were already known from the processing of the vertical channel. To estimate  $V_p/V_s$ , use was made of dipole logs acquired in the deviated well BB-13a in this field. The logs covered the depth interval 284 to 460 m and sonic interval transit times for both compressional and shear waves were recorded. A plot of  $V_p/V_s$  made from the recorded digits (Figure 11) shows an average  $V_p/V_s$  ratio of 2.4 above the reservoir. At the top of the reservoir at 423 m (416 m TVD), the  $V_p/V_s$  ratio decreases to 2.04. An average value of 2.4 was used in the stacking velocity estimation.

After application of geometric spreading compensation and amplitude balancing, statics were calculated. The shot statics for each radial line were the same as those used for the vertical component of that line but the receiver statics were not. The low-velocity surface layer encountered by compressional waves depends on the depth of the water table but, since the velocity of shear waves is independent of fluid content, the shear wave low-velocity layer depends on lithology. Shear wave receiver statics are often much greater than those for the compressional waves, since the depth of the

weathering layer is deeper than the water table and the near-surface  $S$ -wave velocities are very slow.

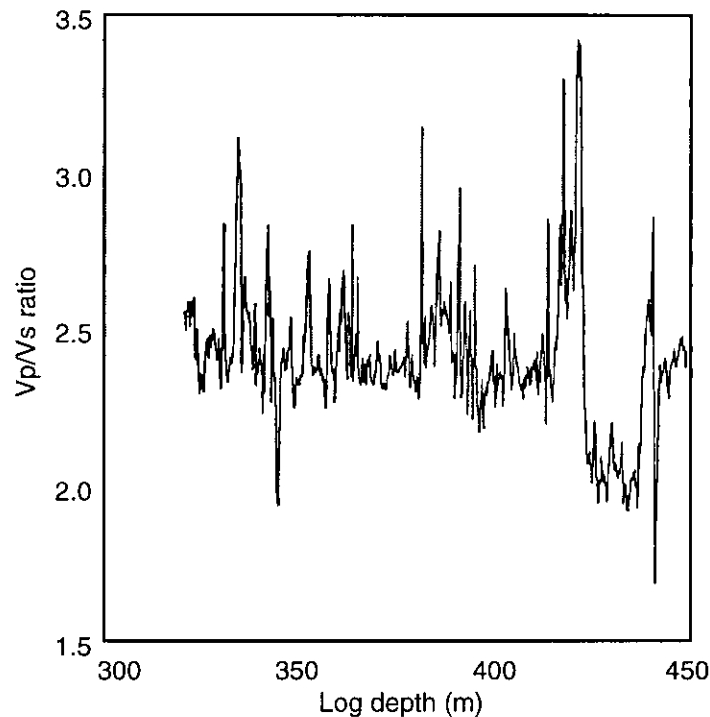


FIG. 11.  $V_p/V_s$  ratio calculated from dipole logs.

Since the 114 receivers were common for each shot line, the receiver static analysis was performed using all the shots in the survey. In order to determine the offsets to be used in this analysis, ray-tracing modelling was done using Sierra software. The model was based on the  $P$ - and  $S$ -wave velocities obtained from the dipole logs for the section in which they were run. For the shallower section  $P$ -wave velocities were obtained from a sonic log obtained at well BB27 (Figure 9) and a  $V_p/V_s$  ratio of 2.4 was used. For the Devonian section, interval velocities calculated during the processing of the data over the D3 pad and a  $V_p/V_s$  ratio of 1.9 were used.

The synthetic shot gather obtained from the modelling is shown in Figure 12. This figure has had AGC applied. The Devonian event is the deepest - 0.85 s at zero offset - and has a very high amplitude on the ungained gather. A clear change in phase of the Devonian event is seen at an offset of 432 m, corresponding to the critical angle for this interface.

Figure 13 shows a raw shot gather of the radial component from line 469. The gather appears noisy and it is very difficult to tell where the converted wave energy might be. A receiver gather, however, (Figure 14), reveals coherent trains of energy, some linear and some with hyperbolic moveout. All shots were used and increasing offsets of 500 m to 1200 m are displayed. The high amplitude peak at about 1.25 s was observed on most of the receiver gathers. Its moveout velocity was calculated to be 1400 m/s, which is the estimated rms velocity of the Devonian reflector, although the Devonian is not expected to be so deep in the section.

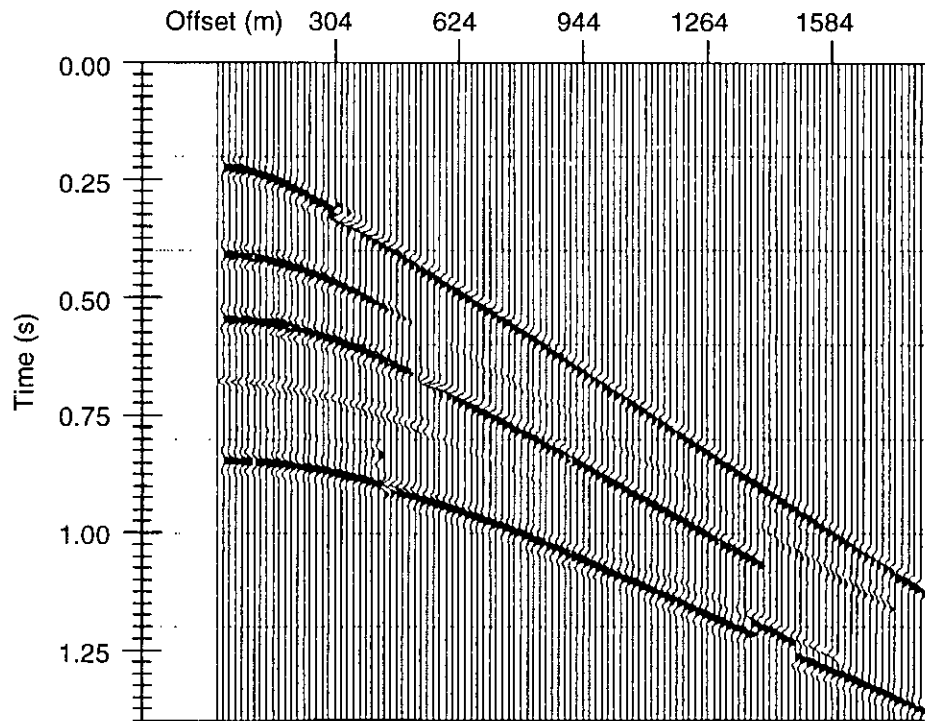


FIG. 12. Synthetic shot gather of  $P$ - $SV$  energy, modelled by ray-tracing.

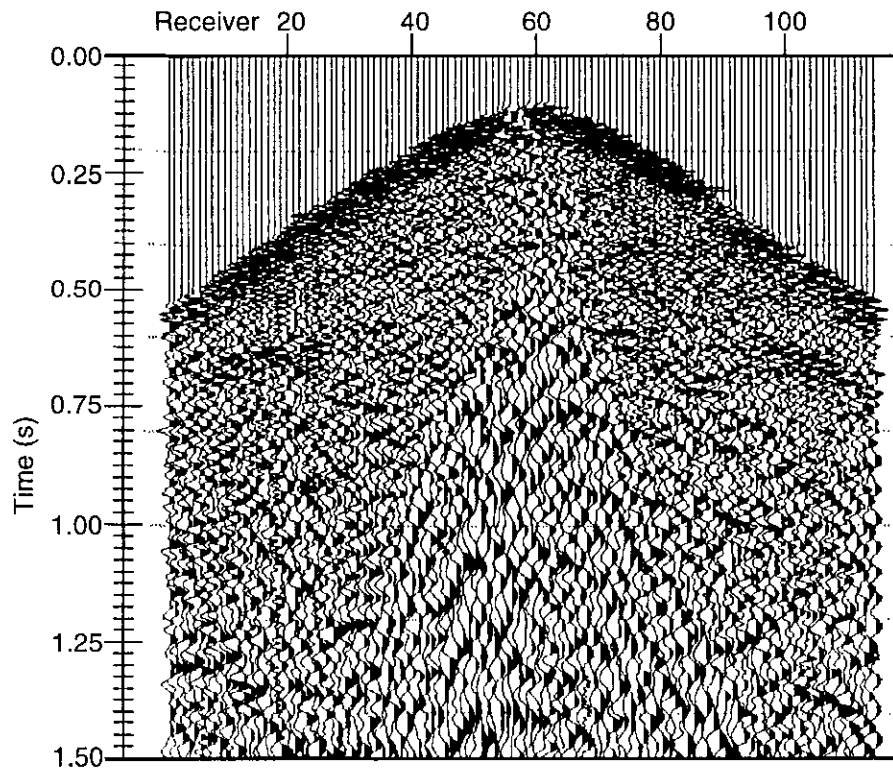


FIG. 13. A raw shot gather of the radial component from line 469.

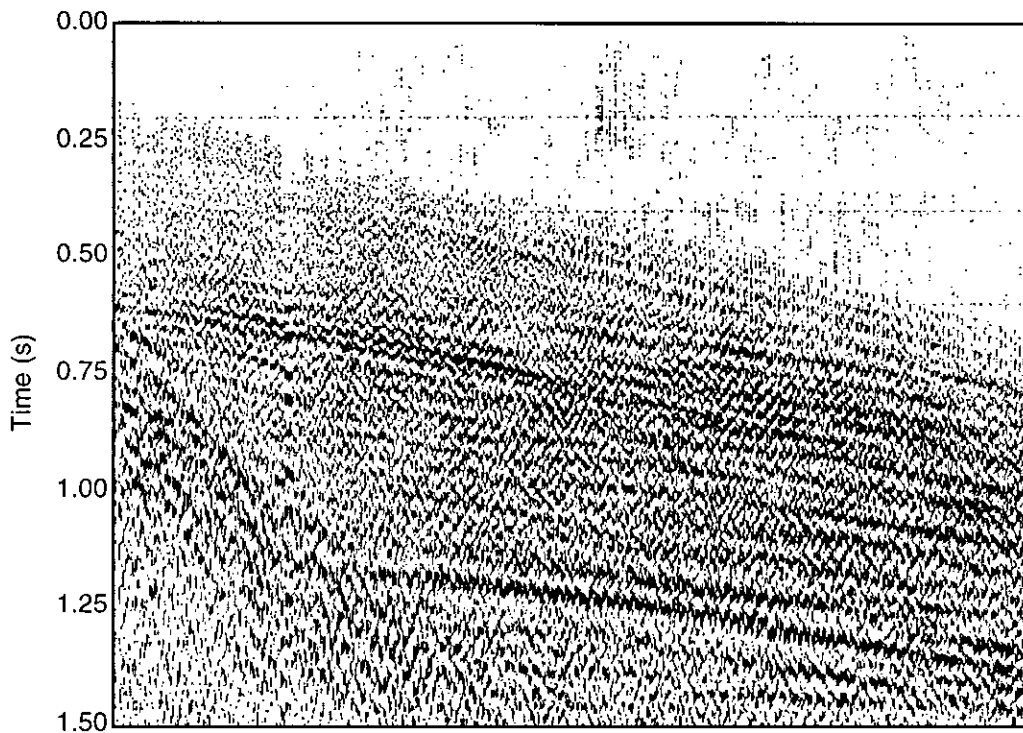
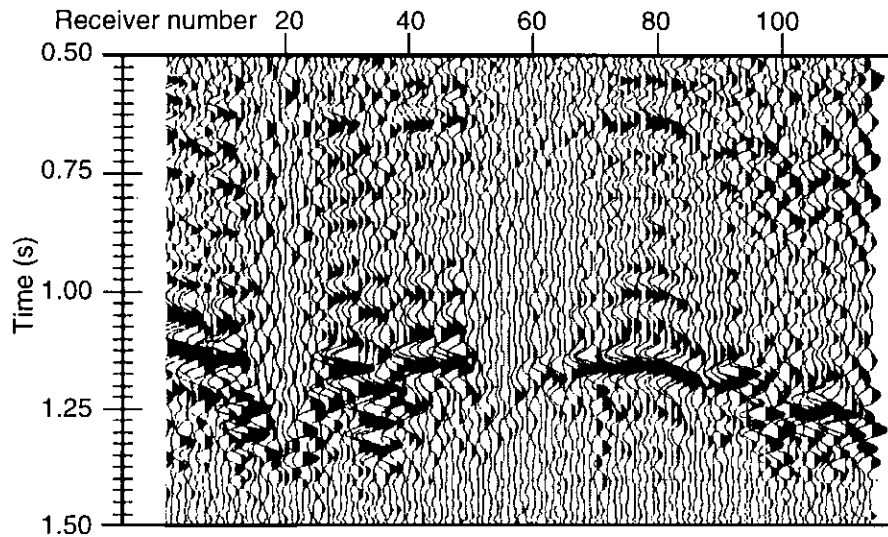


FIG. 14. Receiver gather of the radial component from line 470.

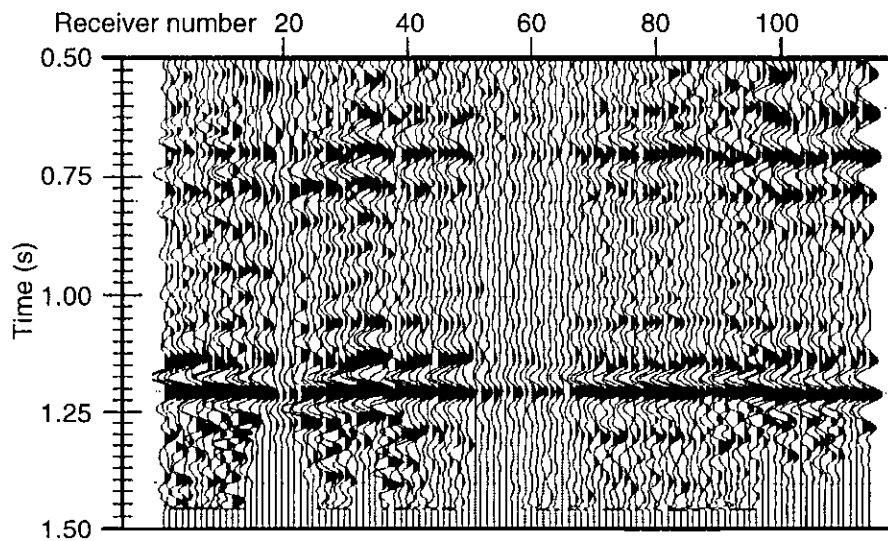
To calculate the receiver statics, all shots and offsets of 500-1200 m (determined from Figure 12) were sorted into receiver gathers. Each gather was NMO-corrected using a constant velocity of 1400 m/s, to flatten the strong event, and stacked. A great range in receiver statics is observed, especially between traces 10 and 30. A first pass at receiver statics was made by hand correlating the strong event on the receiver stack, using NMO-corrected gathers to determine the time of this event when it was not clear on the stacked gathers, e.g., at traces 50-55. The values were found to be very large, ranging between +85 to -162 ms.

The receiver statics calculated in this way were applied to the data and the process repeated. A second pass of statics was calculated using a trim statics routine to align the strong event. These statics were applied to the data and a final receiver stack made for quality control. The original and final stacked receiver gathers are shown in Figure 15. In the lower stack in Figure 15 not only is the strong event aligned but also shallower events, giving confidence in the validity of the calculated receiver statics solution.

Figure 16 shows the same shot gather as in Figure 13 but after applying the receiver statics. We now see coherent energy throughout the record. Any  $P$ - $P$  energy present in the data will now be unaligned since the  $P$ - $P$  receiver statics are different from the  $P$ - $SV$  receiver statics. It is anticipated that, with these receiver statics applied to the data, a better estimate of the  $P$ - $SV$  stacking velocities may be obtained and a usable stacked section generated.



a. Stacked receiver gather



b. Stacked receiver gather after alignment of strong event at 1.2 s.

FIG. 15. The stacked receiver gathers, showing the great receiver statics to be applied to the data.

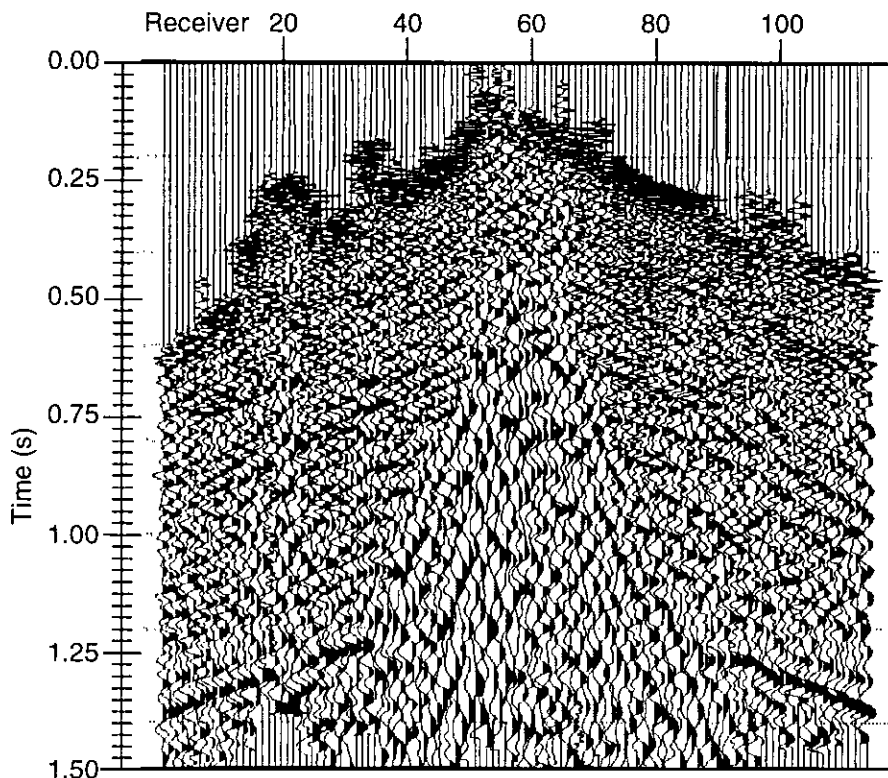


FIG. 16. The same shot gather as in Figure 13 but with receiver statics applied. Coherent events now appear in the data.

## CONCLUSIONS

Two time-lapse 3-D seismic data sets, acquired in 1990 and 1992 for the purposes of reservoir monitoring, had been reprocessed. Differences above the reservoir zone were analysed and found to be minimal. As a consequence, traveltime delays and seismic character differences within the reservoir zone can be ascribed confidently to temporal changes in reservoir conditions caused by the injection of steam into the reservoir. Mapping of such delays and differences can indicate the distribution of the steam and hence contribute to better reservoir management. It is believed that the injection of steam into the reservoir has two effects on the seismic data. The first is an increased interval transit time, due to the lower interval velocities. The second is localised reflectivity changes, where gas present during the production cycle is absent during steaming.

A wavelet was extracted from the seismic data to tie better the synthetic seismograms to the data and for use in 3-D inversion of the data. The inversions show zones of low velocity in the 1990 data which are interpreted to be zones of gas saturation. Low velocity zones on the 1992 data are interpreted to be steamed zones. They are often overlain by tight streaks, which inhibit vertical migration of the steam.

3-C data acquired in 1993 are being processed. Shot gathers indicate the data to be noisy but examination of receiver gathers revealed coherent energy trains in the data. An NMO velocity of 1400 m/s was applied to receiver gathers to flatten a high

amplitude event seen deep in the section on all but the noisiest records. The stacked receiver gathers showed that extremely high receiver statics are necessary. Once these statics are applied to the shot records, converted wave energy becomes apparent on these records. Obtaining a good receiver statics solution gives encouragement that a usable stacked *P-SV* section will be obtained.

## FUTURE PLANS

### 3-C Data

It is hoped that the *P-SV* data from line 470 can be processed into a usable stacked section. Initial attempts have been very disappointing but, with the new receiver statics, improvement is anticipated. Multi-channel filtering will be employed to enhance the converted wave data. Interval transit times, measured from the *P-P* and *P-SV* stacked sections, may be used to calculate  $V_p/V_s$  ratios along the line. Successful processing of the 1993 data will lead to processing of the 1994 follow-up survey (acquired during the production phase) and analysis of the differences observed in the data.

### 3-D AVO

3-D AVO analysis will be undertaken on the two 3-D data sets. The data for analysis will be selected from that area of the survey where fold is greater than 17 and where there is a wide enough range of offsets and azimuths in each CDP. The data will be sorted by azimuth to investigate any azimuthal dependency of the AVO response. Results from the 1990 and 1992 surveys will be compared. AVO modelling will be undertaken to examine the response of the steamed zone.

## ACKNOWLEDGEMENTS

The authors would like to acknowledge the continued support and assistance of Imperial Oil Resources Ltd. in our analysis of Cold Lake seismic data. In particular we appreciate the assistance of Dr. John Eastwood.

## REFERENCES

- Baltenspergen, P. A. and Bay, A. R., 1990, Case study defining the Morrow (Pennsylvanian) using multicomponent seismic data: 60th Ann. Internat. Mtg., Soc. Expl. Geophys., Expanded Abstracts, 167-168.
- Bell, J. S., Price, P. R. and McLellan, P. J., 1994, In-situ stress in the Western Canada Sedimentary Basin *in* Geological Atlas of the Western Canada Sedimentary Basin: C.S.P.G.
- Brown, R. L., McElhatten, W. and Santiago, D. J., 1988, Wavelet estimation: an interpretive approach: *The Leading Edge*, 7, no 12, 16-19.
- Crampin, S., 1985, Evaluation of anisotropy by shear-wave splitting: *Geophysics*, 50, 142-152.
- Dohr, G., 1985, Seismic shear waves, Part B: Applications: Geophysical Press.
- Domenico, S. N., 1984, Rock lithology and porosity determination from shear and compressional wave velocities: *Geophysics*, 49, 1188-1195.
- Eastwood, J., 1993, Temperature-dependent propagation of *P*- and *S*-waves in Cold Lake oil sands: Comparison of theory and experiment: *Geophysics*, 58, 863-872.

- Eastwood, J., Lebel, P., Dilay, A. and Blakeslee, S., 1994, Seismic monitoring of steam-based recovery of bitumen: *The Leading Edge*, **13**, 4, 242-251.
- Harrison, D. B., Glaister, R. P. and Nelson, H. W., 1979, Reservoir description of the Clearwater oil sand, Cold Lake, Alberta, Canada *in* Meyer, R. F. and Steele, C. T., Eds., *The future of heavy crude and tar sands*, 264-279.
- Harrison, M. P., 1992, Processing of P-SV surface seismic data: Anisotropy analysis, dip movcouth and migration: Ph. D. thesis, Univ. of Calgary.
- Isaac, J. H. and Lawton, D. C., 1993, Cold Lake 3-D seismic data analysis: CREWES Research report, **5**, ch 25.
- Laine, E. F., 1987, Remote monitoring of the steam-flood enhanced recovery process: *Geophysics*, **52**, 1457-1465.
- Lazear, G. D., 1984, An examination of the exponential decay method of mixed-phase wavelet estimation: *Geophysics*, **49**, 2094-2099.
- Lynn, H. B. and Thomsen, L. A., 1986, Reflection shear-wave data along the principal axes of azimuthal anisotropy: 56th Ann. Internat. Mtg. Soc. Expl. Geophys., Expanded Abstracts, 473-476.
- Macrides, C. G. and Kanasewich, E. R., 1987, Seismic attenuation and Poisson's ratios in oil sands from crosshole experiments: *J. Can. Soc. Expl. Geophys.*, **23**, 46-55.
- Martin, M. A. and Davis, T. L., 1987, Shear-wave birefringence: a new tool for evaluating fractured reservoirs: *The Leading Edge*, **6**, no. 10, 22-28.
- Nur, A., 1987, Seismic rock properties for reservoir description and monitoring *in* Nolet, G., ed., *Seismic tomography*: D. Reidel Publ. Co.
- Nur, A., Tosaya, C. and Vo-Thanh, D., 1984, Seismic monitoring of enhanced oil recovery processes: 54th Ann. Internat. Mtg. Soc. Expl. Geophys., Expanded Abstracts, 337-340.
- Paulsson, B., Smith, M., Tucker, K. and Fairburn, J., 1992, Characterization of a steamed oil reservoir using crosshole seismology: *The Leading Edge*, **11**, 6, 24-32.
- Tatham, R. H. and McCormack, M. D., 1991, Multicomponent seismology in petroleum exploration: *Soc. Expl. Geophys.*
- Tosaya, C., Nur, A., Vo-Thanh, D. and Da Prat, G., 1987, Laboratory seismic methods for remote monitoring of thermal EOR: *S.P.E. Res. Eng.*, **2**, 235-242.
- Wang, Z. and Nur, A., 1988, Effect of temperature on wave velocities in sands and sandstones with heavy hydrocarbons: *S.P.E. Res. Eng.*, **3**, 158-164.
- Winterstein, D. F., 1986, Anisotropy effects in *P*-wave and *SH*-wave stacking velocities contain information on lithology: *Geophysics*, **51**, 661-672.